Vehicle System Dynamics: International Journal of Vehicle Mechanics and Mobility

Publication details, including instructions for authors and subscription information:
http://www.tandfonline.com/loi/nvsd20

The critical hitch angle for jackknife avoidance during slow backing up of vehicle-trailer systems

Jimmy Chiu[a] & Ambarish Goswami[a]

[a] Honda Research Institute USA, Inc., 425 National Avenue, Suite 100, Mountain View, CA 94043, USA

Published online: 14 May 2014.

To cite this article: Jimmy Chiu & Ambarish Goswami (2014): The critical hitch angle for jackknife avoidance during slow backing up of vehicle-trailer systems, Vehicle System Dynamics: International Journal of Vehicle Mechanics and Mobility, DOI: 10.1080/00423114.2014.909944

To link to this article: http://dx.doi.org/10.1080/00423114.2014.909944

Vehicle System Dynamics, 2014
http://dx.doi.org/10.1080/00423114.2014.909944

Taylor & Francis
Taylor & Francis Group

The critical hitch angle for jackknife avoidance during slow backing up of vehicle–trailer systems

Jimmy Chiu* and Ambarish Goswami

Honda Research Institute USA, Inc., 425 National Avenue, Suite 100, Mountain View, CA 94043, USA

(*Received 6 February 2014; accepted 23 March 2014*)

We set out to answer the question: At what hitch angle does it become impossible for a vehicle and trailer to continue to backing up without getting into a jackknife? Jackknifing during backing up of trailers occurs when the hitch angle increases to a point such that the vehicle and trailer fold together about the hitch point like a jackknife. If the backward motion is continued, the jackknife effect progressively worsens, until the vehicle and trailer are in physical contact with each other. Jackknifing can result in traffic disruptions and wasted time, and can potentially cause damage or personal injury. Our goal is to analytically determine the 'critical hitch angle' (θ_{cr}), the hitch angle threshold beyond which a continued reverse motion causes an *inescapable* jackknifing. In this paper, we provide a formal definition of θ_{cr} for slow backing up of vehicle–trailer systems on a level solid surface, beyond which the vehicle must stop backing up and revert to forward motion in order to escape from jackknifing. The critical hitch angle is sub-categorised into *Absolute* ($\theta_{cr,a}$) and *Directional* ($\theta_{cr,d}$) critical hitch angles depending on the operating constraints and vehicle steering objectives. One solution for θ_{cr} is posed as a numerical solution to the steady-state conditions of the dynamic equations. The effects of such hitch angle limitations are demonstrated through simulation. Also, a warning system making use of the θ_{cr} is proposed. Such warning systems can assist drivers in avoiding jackknifing while backing up a vehicle–trailer system.

Keywords: critical hitch angle; pull forward; point of impasse; jackknife; trailer; trailer steering; backing up; hitch angle; numerical minimization

1. Introduction

We set out to answer the question: At what hitch angle does it become impossible for a vehicle and trailer to continue backing up without getting into a jackknife configuration? Jackknifing during backing up of trailers occurs when the hitch angle increases to a point such that the vehicle and trailer fold together about the hitch point like a jackknife, hence the name. If the backward motion is continued, the jackknife effect progressively worsens, eventually resulting in physical contact between the vehicle and the trailer. The lack of direct control of the trailer can result in annoyance and wasted time to the driver and in the worst case scenario, can cause physical damage or injury.

In the traditional literature, a kinematic threshold based on the relative orientation between the vehicle and trailer is used as the condition for jackknifing,[1–4] however, it is ad hoc and not based on any analysis. This approach has limited benefit because it does not give us any

*Corresponding author. Email: jchiu@hra.com

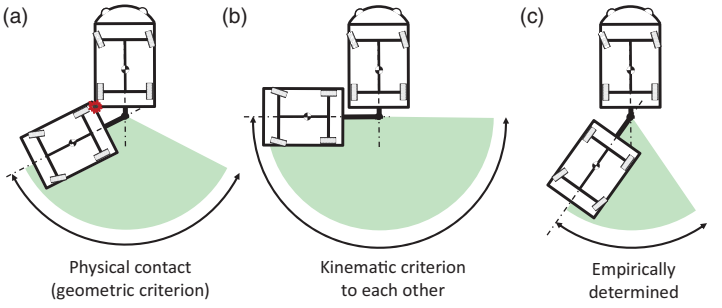

Figure 1. Critical hitch angle can be based on (a) actual physical contact between a vehicle and trailer, (b) a kinematic criteria where the vehicle and trailer are perpendicular or (c) an empirically defined threshold. The green-shaded area in each case shows the permissible hitch angle range in which the trailer centreline can lie.

indication of how such a condition might change with a variation in kinematic and dynamic vehicle–trailer parameters. In this paper, we would like to determine the conditions that lead to an *inescapable* jackknife under continued reverse motion. In particular, our interest is to find the onset of inescapable jackknifing because such an information can be used to warn drivers of the impending problems. For slow backing up of a vehicle–trailer system, we seek to analytically find the *critical hitch angle* θ_{cr}, beyond which *the vehicle must stop backing up and revert to forward motion in order to extricate itself from a jackknife configuration*.

The idea that there exists some threshold condition, the crossing of which necessitates forward motion to prevent jackknifing exists in the literature.[1,2,5–8] However, mathematical models only exist for single-axle trailer systems, which uses the assumption of no-slip motion. In [9], the critical hitch angle for a single-axle trailer is not explicitly referred to, but the authors demonstrate that based on an initial hitch angle and fixed steering angle, certain configurations result in an increasing hitch angle and eventual jackknife, while others decrease the hitch angle. It is common to base backing up warning and control systems on some hitch angle limitation, whether derived by physical contact constraints of the system as shown in Figure 1(a),[2,10] or when the hitch angle is $\pm 90^\circ$ as depicted in Figure 1(b).[4,11–13] Empirical approaches to determining the hitch angle limitation have also been demonstrated in [8,14,15], suggesting a hitch angle range less than $\pm 90^\circ$ is necessary, shown in Figure 1(c).

Although empirical approaches to determining a critical hitch angle have been utilised in practice, a literature search for the critical hitch angle for backing up of trailers shows that the concept is commonly referred to without indication of how such a threshold can be calculated analytically. In [16], the authors state that a jackknife event is likely if the hitch angle is greater than 34°, while the authors in [17] specify a hitch angle limitation of 45° to prevent the possibility of jackknifing. In both cases, the hitch angle limits are significantly lower than the traditional 'kinematic' jackknife criteria of 90°, though each value is specific to system geometry, parameters and loading conditions. The authors of [18] suggest the use of a 'Backing up jackknife detection and warning system', indicating visually or aurally to the driver about the system's proximity to a 'predetermined maximum critical hitch angle', though no explicit solution of the determination methodology for such an angle is provided. While this result does attempt to answer the question of the threshold on the hitch angle where jackknifing begins, empirical approaches do not lend well to variations in parameters such as trailer loading conditions, as demonstrated in [19], where the controllable set of hitch angles is set to $(-90^\circ + \epsilon) \leq \theta \leq (90^\circ - \epsilon])$, where $\epsilon > 0$ is an angle determined empirically such that the controllable set is less than $\pm 90^\circ$. With an abundance of control strategies available for backing up control of trailers,[2,6,7,20–27] it is important that there should exist a

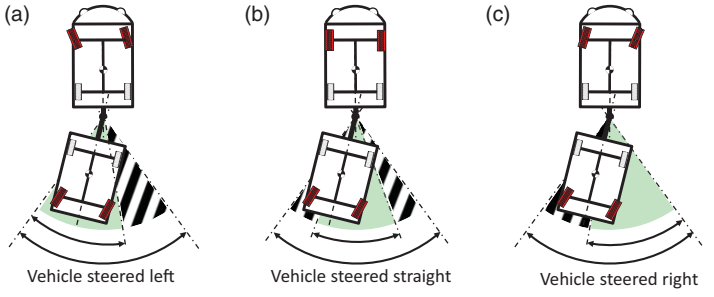

Figure 2. Our proposed definition of critical hitch angle takes into consideration the intent of the driver by capturing a desired direction based on the vehicle steering angle. The critical hitch angle has an absolute value (regardless of vehicle steering, shown in dashed area) and directional value (based on current vehicle steering, shown in green), and have both an upper and lower limits. As the vehicle steering changes from steered left (a) to centred (b) to steered right (c), the range of hitch angles bounded by the directional critical hitch angle threshold also shifts from left to right.

mathematical approach for the determination of the critical hitch angle. Note that the analytical solution to the critical hitch angle may exceed the hitch angle at which physical contact occurs, in which case the physical contact criteria supersedes any other condition as the maximum allowable hitch angle. For example, consider a vehicle and trailer layout with some nominal hitch length, trackwidth and wheelbase. If the body of the vehicle and trailer is very wide, then physical contact between the bodies occurs at a small hitch angle. This contact occurs at the small hitch angle regardless of kinematic and dynamic properties of the vehicle and trailer.

A backup controller is presented in [3] which demonstrates that under a backing up turn manoeuver, the desired hitch angle is 'stabilised' with an upper and lower bounded hitch rate, that is, the steering input of the vehicle is manipulated in a way such that the hitch angle is indirectly controlled. Any deviation from the desired hitch angle can be controlled with steering inputs, hence we can view the hitch angle as a controllable state when operating within the mechanical limitations of the vehicle–trailer. Conversely, when the system exceeds the critical hitch angle threshold, the controllability of the hitch angle by actuation of the steering angle is lost. In the case that both vehicle and trailer have independent steering, when the critical angle threshold is exceeded, there exists no combination of vehicle or trailer steering inputs such that the hitch angle can decrease when backing up the system. At this point, the only way to decrease the hitch angle is to drive the vehicle forward.

Being able to reduce the hitch angle at any point during an arbitrary backing up motion is essential to maintaining control over the trailer. When the ability to decrease hitch angle is lost for continued backing up motion, the critical hitch angle threshold has been exceeded. In this paper, we outline the conditions on the vehicle and trailer steering inputs (both steered and unsteered trailers will be considered for long-wheelbase trailers) and initial hitch angles which maintain the ability to reduce hitch angle, demonstrating the thresholds beyond which a reduction of hitch angle is not possible under backing up, shown in Figure 2. In this figure, we show the potential range of allowable hitch angles for a long-wheelbase trailer with steering for (a) when the vehicle is steered to the left, (b) when the vehicle steering is straight and (c) when the vehicle is steered to the right. Note that in each case, the feasible range of hitch angles in the solid-shaded area is changing as the vehicle steering angle changes, since the path of the vehicle is being changed. This range is bounded by the *Directional critical hitch angles*, which is dependent on the vehicle heading direction. The range of hitch angles spanned by the stripe-shaded area is invariant of the vehicle steering angle, which is bounded

by the *Absolute critical hitch angles*. Both absolute and directional critical hitch angles are formally defined in the following section.

We also provide a formal definition of critical hitch angle both for the traditional single-axle trailer, as well as long-wheelbase dual-axle trailer with a fixed front axle and steerable rear axle. Unlike other dual-axle trailers where the front axle is a dolly, the fixed front axle in our study provides some interesting constraints to the motion and requires steering in order to turn without significant tyre scrub. We consider both steered and unsteered trailers, examining the critical hitch angle for each case and looking at the controllable set for each case. Note that for dual-axle steered trailers, we analyse the hitch angle limit of the vehicle–trailer assuming that the driver controls only the vehicle steering angle, and the trailer steering actuation is handled by a control system.

The scope of this work is limited to slow speed backing up motion, thus dynamic effects of the motion are assumed to be negligible. Furthermore, the examples presented assume tyre–surface models representative of tyres on non-deformable road surfaces. Common examples where non-deformable road surface may be applicable are semi-trailers reversing into a docking/loading station or personal trailers backing up in a driveway or parking area. While we present results for the non-deformable road surface models, we show how such an analysis could be extended to deformable surface contacts, such as farming, agricultural and off-road applications of vehicle–trailers.

In Section 2, we present the formal definition of the critical hitch angle for vehicle–trailer systems, identifying concepts such as absolute and directional criteria for the critical hitch angle. Section 3 provides a solution for the critical hitch angle for single-axle trailers, with comparison of our approach to an existing kinematic solution (which assumes no tyre slip). In Section 4, we extend the solution of critical hitch angle to vehicle–trailer systems with a long-wheelbase trailer, where the trailer has steering on its rear axle. The main contributions of this paper are an analytical algorithm for solving the critical hitch angle in the presence of tyre slip.

2. The 'critical hitch angle' θ_{cr}

Here we present a formal definition of the 'critical hitch angle' (θ_{cr}) for slow speed backing up of trailers, which is valid for both single-axle and dual-axle trailers. First we introduce the hitch control space [27] which is the 3D Euclidean space spanned by three variables: the vehicle steering angle δ_v , the trailer steering angle δ_t, and the hitch angle θ, as shown in Figure 3. In the case where the trailer has no steering, the hitch control space lies on the 2D plane spanning δ_v and θ. Recall that we cannot directly control θ; δ_v and δ_t are the only available inputs to indirectly control θ when the trailer has steering capability. For a trailer without steering, only δ_v is available to indirectly control θ. This state is referred to as 'underactuated' [28] as we cannot directly control θ. Recall also that the ability to reduce θ is critical to maintaining control over the trailer.

During backing up, some combinations of δ_v and δ_t will result in $\dot{\theta} > 0$, in which case θ will increase. For other combinations, $\dot{\theta} < 0$, thus θ will decrease. If we know the sign of $\dot{\theta}$ for each $[\delta_v, \delta_t]$ combination, then we can determine if the hitch angle magnitude is decreasing, that is, if $|\theta| \to 0$ for the given steering angle pair. In the case that trailer steering is not available, we want to determine the sign of $\dot{\theta}$ for each δ_v to determine if $|\theta| \to 0$.

We call the critical hitch angle θ_{cr} as *the hitch angle beyond which there exists no steering angles* δ_v *and/or* δ_t *that reduce the hitch angle magnitude*. If θ_{cr} is exceeded, then the only way to reduce $|\theta|$ would be to stop backing up and to revert to forward driving. For the case of

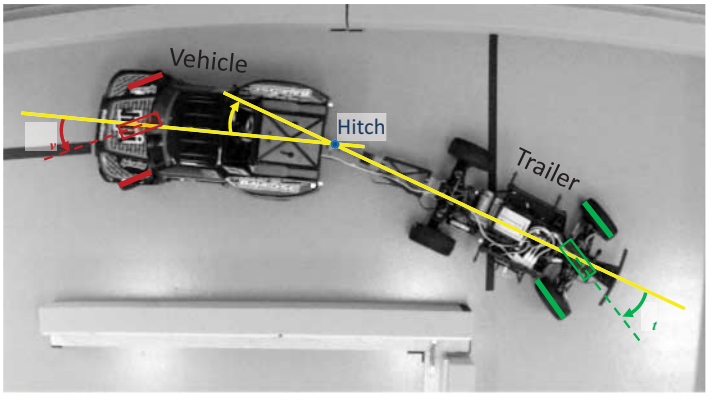

Figure 3. Definition of the three parameters spanning the hitch control space [27]: vehicle steering angle δ_v, trailer steering angle δ_t and hitch angle θ for a vehicle with a long-wheelbase steered trailer. Note that δ_v is clockwise–positive, thus in the photo is shown with negative steering angle. The steering angles δ_v and δ_t are taken to be the average angles of the left and right sides for each respective axle.

an unsteered trailer ($\delta_t = 0$ always), the definition of θ_{cr} simplifies to *the hitch angle beyond which there exists no vehicle steering angle* δ_v *that reduces the hitch angle magnitude*.

When trailer steering is present, the critical hitch angle θ_{cr} can be classified into two sub-categories:

(1) *Absolute* critical hitch angle ($\theta_{cr,a}$): This is the hitch angle threshold beyond which no possible combination of (δ_v, δ_t) can reduce the hitch angle magnitude during backing up.
(2) *Directional* critical hitch angle ($\theta_{cr,d}$): This is the hitch angle threshold beyond which, for a given δ_v , no possible δ_t can reduce the hitch angle magnitude during backing up.

To explain the concept of absolute and directional critical hitch angles schematically, we present a series of figures in this section, each with incrementally more information and depth than the previous. The figures culminate in the overall picture of the critical hitch angle and its utility in Figure 7, followed by an example with real simulation results in Figure 14. The figures are created in such a way to walk the reader through the reasoning and derivation of critical hitch angle step by step. We consider various operating points, that is, the combinations of current hitch angles θ and trailer steering angles δ_t for a given vehicle steering angle δ_v in order to determine if backing up in such configurations result in increasing or decreasing $|\theta|$.

The $\theta_{cr,a}$ and $\theta_{cr,d}$ have both upper (denoted by a superscript $^+$) and lower (denoted by a superscript $^-$) thresholds that define the range of hitch angles where the ability to reduce $|\theta|$ is retained, as previously shown in Figure 2 by the left and right bounds of the hitch angle ranges. If the threshold is exceeded, it is not possible to reduce the magnitude of the hitch angle in backing up motion. In Figure 4, we schematically show how the upper and lower thresholds of $\theta_{cr,a}$ and $\theta_{cr,d}$ might vary in the $\theta - \delta_t$ space as δ_v is changed. Starting with $\delta_v = 0^\circ$ in Figure 4(a), we can see the shaded area bounded by $\theta^+_{cr,d}$ and $\theta^-_{cr,d}$. As δ_v increases to 10° (Figure 4(b)) and 30° (Figure 4(c)), the shaded area shifts downward. As the vehicle steering angle changes, the range of initial hitch angles $|\theta|$ can be reduced shifts. However, $\theta_{cr,a}$ remains constant since it is determined by the upper and lower limits of δ_v. Effectively, $\theta_{cr,a}$ is the value of critical hitch angle at the extremum values of both vehicle and trailer steering angles. For example, $\theta^+_{cr,a}$ occurs at minimum δ_v and minimum δ_t (noting that minimum is the most negative value, not the minimum magnitude of steering angle).

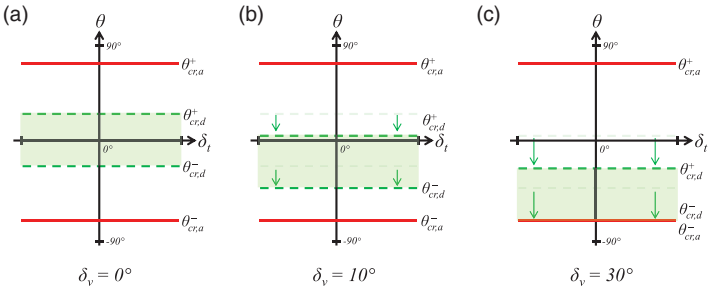

Figure 4. As steering angle increases (from $\delta_v = 0^\circ$ in (a), to 10° in (b) and 30° in (c)), $\theta^-_{cr,d}$ and $\theta^+_{cr,d}$ shift downward towards negative θ. This is shown by the shift of the shaded area between $\theta^-_{cr,d}$ and $\theta^+_{cr,d}$, marked by downward arrows from the prior steering angle to the subsequent steering angle. The $\theta^-_{cr,d}$ at the maximum δ_v is equal to $\theta^-_{cr,a}$. Similarly, as δ_v becomes more negative, $\theta^-_{cr,d}$ and $\theta^+_{cr,d}$ shift to the top. Also, $\theta^+_{cr,d}$ at minimum δ_v is equal to the upper $\theta^+_{cr,a}$.

If the initial hitch angle θ_0 is larger than $\theta^+_{cr,a}$, there would not exist any steering angle that can result in decreasing hitch angle magnitude with backing up motion. In this case, it is necessary to pull the vehicle forward to reduce the hitch angle. Note that since $\theta_{cr,a}$ is simply the $\theta_{cr,d}$ at the maximum and minimum steering limits of the vehicle, we can deduce that

$$|\theta_{cr,d}| \leq |\theta_{cr,a}|. \tag{1}$$

Now let us consider specific operating points within the directional critical hitch angle limits, that is, $\theta^-_{cr,d} < \theta < \theta^+_{cr,d}$. Figure 5(a) shows some example trajectories of the operating point in the $\theta - \delta_t$ space for various initial operating points. Note that not all operating points above $\theta^-_{cr,d}$ must go towards decreasing $|\theta|$ (towards $\theta = 0$). This is because the directional critical hitch angle simply requires the existence of *some* feasible δ_t (within the steering limitations of the trailer) that reduces the hitch angle magnitude, specifically that at least one value of $\delta_{t,\min} \leq \delta_t \leq \delta_{t,\max}$ that will reduce $|\theta|$ exists. Another way to state this is that $\theta^-_{cr,d} < \theta < \theta^+_{cr,d}$ satisfies the *necessary but not the sufficient condition* for reduction in hitch angle magnitude. For example, a vehicle–trailer backing up at operating point B′ does not result in a reduction of hitch angle magnitude, as the trajectories point away from $\theta = 0$. However, it is possible to change δ_t to move the operating points from B′ to B such that the hitch angle magnitude does reduce with backup motion. Any point below $\theta^-_{cr,d}$ in (a) (e.g. points A, A′, C and D) increases $|\theta|$, eventually resulting in jackknifing. No change of δ_t (even instantaneously or while stationary, moving from points A to A′) will result in decreasing $|\theta|$ for $\delta_v = 0^\circ$.

When the initial hitch angle θ_0 satisfies $\theta^-_{cr,a} \leq \theta_0 \leq \theta^-_{cr,d}$, we can do one of two things to avoid a jackknife: (a) stop backing up and pull forward or (b) increase δ_v to lower the $\theta_{cr,d}$ such that $\theta^-_{cr,d} < \theta_0 < \theta^+_{cr,d}$, as shown in Figure 5(b). Here we show that by increasing δ_v , points A′ and A now both lie above $\theta^-_{cr,d}$, thus there exists some δ_t such that backing up results in a reduction of hitch angle magnitude. We now have a formal definition of $\theta_{cr,a}$ and $\theta_{cr,d}$, however no method for determining these thresholds and more importantly what specifically happens between $\theta^-_{cr,d}$ and $\theta^+_{cr,d}$. The following section addresses how to find the upper and lower values of $\theta_{cr,a}$, $\theta_{cr,d}$ and how to determine the direction of the hitch angle under backing up motion for any operating point in the hitch control space.

Steady state and its relationship with the critical hitch angle θ_{cr}

In Figure 5 , we schematically showed a few possible hitch angle trajectories in the $\theta - \delta_t$ space. For some initial hitch angles θ_0, a backing up motion results in $\dot{\theta} > 0$, which increase

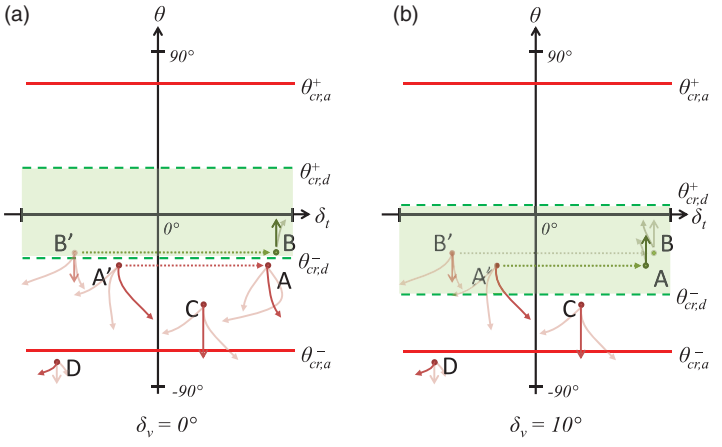

Figure 5. We now consider individual points in the region bounded by the green-shaded region satisfying $\theta^-_{\mathrm{cr,d}} < \theta < \theta^+_{\mathrm{cr,d}}$. There exists at least *some* combinations of δ_v and δ_t such that the hitch angle goes towards zero. However, this is not a sufficient condition, so not all points in the shaded region between $\theta^-_{\mathrm{cr,d}} < \theta < \theta^+_{\mathrm{cr,d}}$ result in $\theta \to 0$. For example, point B′ in (a) does not reduce $|\theta|$, however for the same θ with a different δ_t, shown by point B, results in $\theta \to 0$. As δ_v increases (depicted by subfigure (b)), both $\theta^+_{\mathrm{cr,d}}$ and $\theta^-_{\mathrm{cr,d}}$ move downward, as we already saw in Figure 4. By doing so, points A and A′ now fall in the area bounded by $\theta^+_{\mathrm{cr,d}}$ and $\theta^-_{\mathrm{cr,d}}$. It is possible to adjust δ_t such that $|\theta|$ can be decreased, for example, moving from points A′ to A.

θ. For other values of θ_0, a backing up motion will result in $\dot{\theta} < 0$, which decreases θ. It therefore seems logical that there is a value of θ_0 for which $\dot{\theta} = 0$, and for which θ remains constant. In fact, this steady-state value of θ, denoted by θ_{ss}, marks the boundary between the regions corresponding to $\dot{\theta} > 0$ and $\dot{\theta} < 0$.

We make the assumption that for any given δ_v and δ_t , there exists a θ_{ss} corresponding to $\dot{\theta} = 0$. If we begin at this steady-state value (i.e. $\theta_0 = \theta_{\mathrm{ss}}$) and the vehicle–trailer system is not subject to any external perturbations, $\dot{\theta} = 0$ and thus θ is constant. Furthermore, we assume that this θ_{ss} is a boundary point between $\dot{\theta} < 0$ and $\dot{\theta} > 0$, that is, $\dot{\theta}$ is positive or negative on either side of $\theta = \theta_{\mathrm{ss}}$.

By solving the vehicle–trailer dynamic equations for this steady state, we are able to obtain the boundary between increasing and decreasing hitch angles, shown schematically for $\delta_\mathrm{v} = 10^\circ$ in Figure 6. Here, we see a curve of steady-state solutions for various δ_t , shown as the blue dash-dot-dot line between $\theta^+_{\mathrm{cr,d}}$ and $\theta^-_{\mathrm{cr,d}}$. The curve is defined by steady-state operating points that satisfy $\dot{\theta} = 0$. Any operating point above this curve results in $\dot{\theta} > 0$ and conversely any point below the curve corresponds to $\dot{\theta} < 0$. As δ_v changes, the steady-state solution curve also shifts, bounded by $\theta^+_{\mathrm{cr,d}}$ and $\theta^-_{\mathrm{cr,d}}$.

In order to maintain control of the trailer during backing up, we should have at least one operating point in the $\theta - \delta_\mathrm{t}$ space that leads to $|\theta| \to 0$. If the initial hitch angle $\theta_0 < 0$, then the goal is to ensure that an operating point corresponding to $\dot{\theta} > 0$ exists. On the other hand, if $\theta_0 > 0$, we need to know the operating points such that $\dot{\theta} < 0$. Figure 7(a) shows the possible operating points in the $\theta - \delta_\mathrm{t}$ space for $\delta_\mathrm{v} = 0^\circ$ corresponding to a decreasing $|\theta|$, shown in the yellow stripe-shaded region. If the operating point lies inside this yellow stripe-shaded area, then continued backing up motion results in a decreasing $|\theta|$. A similar area is shown for $\delta_\mathrm{v} = 10^\circ$ in Figure 7(b), where the yellow stripe-shaded area below $\theta = 0$ is larger. If the initial operating point does not lie in this yellow stripe-shaded area and the goal is to reduce $|\theta|$, then either or both δ_v and δ_t need to be adjusted such that the operating point is moved into the yellow stripe-shaded area.

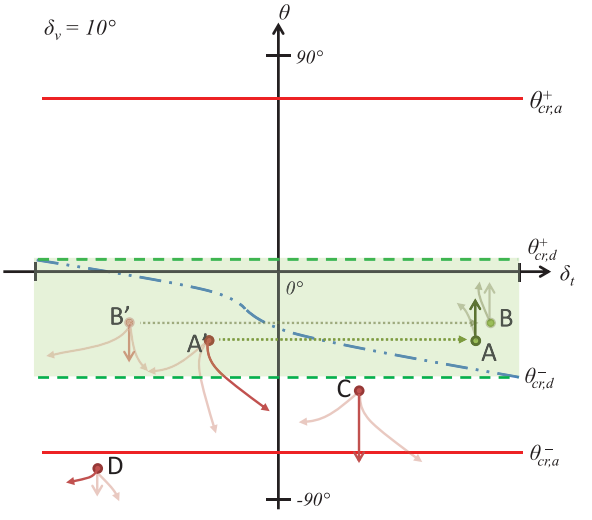

Figure 6. We have identified that some but not all points in the green-shaded area bounded by $\theta^-_{\mathrm{cr,d}} < \theta < \theta^+_{\mathrm{cr,d}}$ reduce $|\theta|$, whereas other points increase $|\theta|$. There must exist a boundary value which separates $\dot{\theta} > 0$ and $\dot{\theta} < 0$. Using the steady state θ at each δ_{t} (for $\delta_{\mathrm{v}} = 10^\circ$, fixed), we know precisely where the operating point does not change hitch angle (i.e. $\dot{\theta} = 0$). The curve of the steady-state solutions (shown in blue dash-dot-dot) signifies the threshold between increasing and decreasing $|\theta|$. For a fixed δ_{v}, the controller needs adjust δ_{t} such that the operating point is above or to the right of the blue dash-dot-dot line in order to result in $\dot{\theta} > 0$.

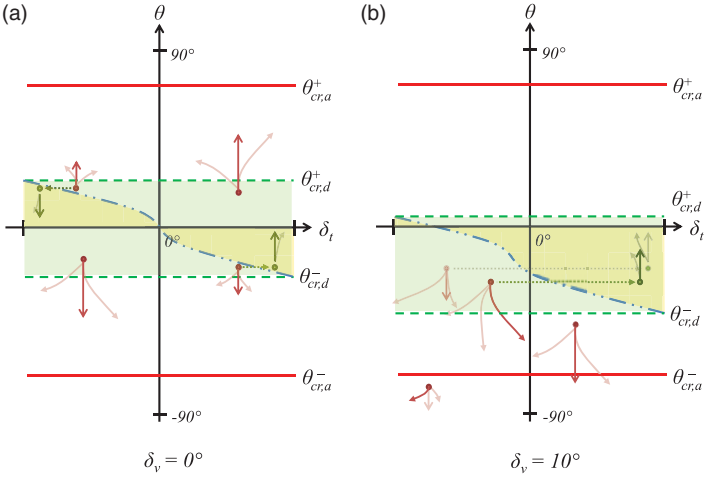

Figure 7. Depending on if the initial hitch angle is positive or negative, the areas of the $\theta - \delta_{\mathrm{t}}$ space which result in hitch magnitude reduction are shown in the yellow stripe-shaded area. If the operating point is located outside of these yellow stripe-shaded areas, then the driver must adjust the vehicle steering angle, or the controller must adjust δ_{t}, such that the operating point moves into this area. For $\delta_{\mathrm{v}} = 0^\circ$ and a symmetric vehicle–trailer shown in subfigure (a), the steady-state solutions curve is symmetric and of opposite sign about the zero hitch angle axis. Changing vehicle steering angle to $\delta_{\mathrm{v}} = 10^\circ$ (shown in subfigure (b)) results in both a vertical and lateral shift of the steady solutions curve. Furthermore, the shape of the curve is not necessarily the same for a non-zero steering angle compared to that of $\delta_{\mathrm{v}} = 0^\circ$. In subfigure (b), the area of positive hitch angles that can reduce $|\theta|$ is reduced, whereas the area of negative hitch angles that can reduce $|\theta|$ is increased. If δ_{v} is further increased, the $\theta^+_{\mathrm{cr,d}}$ can be less than zero, which means it is no longer possible to back up and reduce $|\theta|$ for any initial hitch angle greater than zero without changing δ_{v} first.

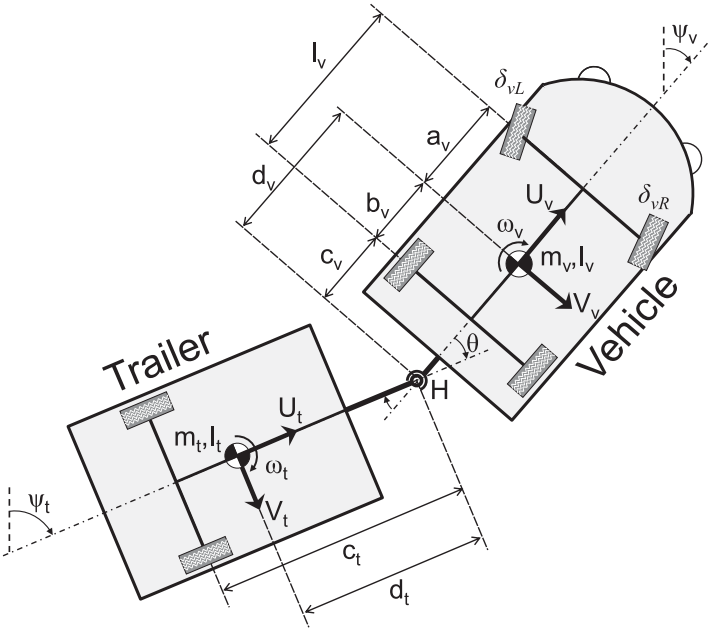

Figure 8. Model parameters for a vehicle–trailer system consisting of a single-axle trailer. The vehicle has front-steered wheels and the trailer is unsteered. The left and right steering angles of the vehicle are denoted by $\delta_{v\mathrm{L}}$ and $\delta_{v\mathrm{R}}$, which are determined by Ackermann geometry, with average value δ_{v}. The vehicle and trailer are connected via a revolute hitch joint with its location denoted by H.

The method for finding the critical hitch angle is therefore achieved by solving for the steady solution θ_{ss} where $\dot{\theta} = 0$. We utilise this approach to develop a solver algorithm for the critical hitch angle in the subsequent sections, beginning with a simpler case of a vehicle coupled to a single-axle unsteered trailer. Since a kinematic solution exists for the single-axle trailer case, we use it as a baseline to compare with the results generated using our steady-state solution approach. Subsequently, we extend the result and solver algorithm to the case of a vehicle with a long-wheelbase dual-axle trailer, where no existing results are available. We show that it is possible to calculate the critical hitch angle for vehicle–trailer systems whilst factoring in effects of tyre slip, which are necessary for the long-wheelbase trailer.

3. Critical hitch angle for a single-axle trailers

3.1. *Single-axle trailer model*

In order to analytically determine the θ_{cr}, we need to define a vehicle–trailer model and then find the steady-state solution of hitch angle for each δ_{v} . The single-axle unsteered trailer is shown in Figure 8. The description and units of each of the vehicle–trailer parameters shown in Figure 8 are defined in Table 1.

The equations of motion for this system are given by

$$m_{\mathrm{v}}(\dot{U}_{\mathrm{v}} - V_{\mathrm{v}}\omega_{\mathrm{v}}) + m_{\mathrm{t}}(\dot{U}_{\mathrm{t}} - V_{\mathrm{t}}\omega_{\mathrm{t}})\cos\theta - m_{\mathrm{t}}(\dot{V}_{\mathrm{t}} + U_{\mathrm{t}}\omega_{\mathrm{t}})\sin\theta = \sum F_{xv} + \sum F_{xt}\cos\theta - \sum F_{yt}\sin\theta, \quad (2)$$

Table 1. Vehicle and single-axle trailer parameter definitions.

Parameter	Description	Units
a_v	Longitudinal distance from vehicle CoM to front axle	m
b_v	Longitudinal distance from vehicle CoM to rear axle	m
c_v	Longitudinal distance from vehicle rear axle to hitch	m
l_v	Vehicle wheelbase ($l_v = a_v + b_v$)	m
d_v	Longitudinal distance from vehicle CoM to hitch	m
c_t	Longitudinal distance from trailer axle to hitch	m
d_t	Longitudinal distance from trailer CoM to hitch	m
m_v	Vehicle mass	kg
m_t	Trailer mass	kg
I_v	Vehicle yaw moment of inertia about CoM	kg m^2
I_t	Trailer yaw moment of inertia about CoM	kg m^2
δ_v	Vehicle steering angle (front), clockwise-positive	$^\circ$
$C_{\alpha,vf}$, $C_{\alpha,vr}$	Vehicle lateral cornering stiffness (front, rear)	N/$^\circ$
$C_{\alpha,t}$	Trailer lateral cornering stiffness	N/$^\circ$

$$m_v(\dot{V}_v + U_v\omega_v) + m_t(\dot{U}_t - V_t\omega_t)\sin\theta + m_t(\dot{V}_t + U_t\omega_t)\cos\theta = \sum F_{yv} + \sum F_{xt}\sin\theta + \sum F_{yt}\cos\theta, \tag{3}$$

$$I_v\dot{\omega}_v + d_v \cdot m_v(\dot{V}_v + U_v\omega_v) = \sum M_v + d_v \cdot \sum F_{yv}, \tag{4}$$

$$I_t\dot{\omega}_t - d_t \cdot m_v[(\dot{U}_v - V_v\omega_v)\sin\theta - (\dot{V}_v + U_v\omega_v)\cos\theta] = \sum M_t - d_t \cdot \left(\sum F_{xv}\sin\theta - \sum F_{yv}\cos\theta\right). \tag{5}$$

It is assumed that the only external contact forces acting on the vehicle and trailer are due to the tyre–ground interaction forces. In this assumption, we make no choice on the possible tyre–ground contact models that can be used. The tyre forces and moments resulting from the these forces about the vehicle and trailer centre of mass (CoM) for the single-axle unsteered trailer are given by

$$\sum F_{xv} = F_{xv,f}\cos\delta_v - F_{yv,f}\sin\delta_v + F_{xv,r}, \tag{6}$$

$$\sum F_{yv} = F_{xv,f}\sin\delta_v + F_{yv,f}\cos\delta_v + F_{yv,r}, \tag{7}$$

$$\sum M_v = a_v(F_{xv,f}\sin\delta_v + F_{yv,f}\cos\delta_v) - b_v \cdot F_{yv,r}, \tag{8}$$

$$\sum F_{xt} = F_{xt}, \tag{9}$$

$$\sum F_{yt} = F_{yt}, \tag{10}$$

$$\sum M_t = -(c_t - d_t) \cdot F_{yt}. \tag{11}$$

In this paper, we limit the scope of our analysis on single-axle unsteered trailers (note that the vehicle is still steered), however, the approach is still valid for steered trailers provided the tyre force models calculate the appropriate lateral forces in the presence of steer angle.

Determination of θ_{cr} in the presence of slip requires a vehicle–trailer model that allows for tyre slip and the resulting tyre forces due to the tyre–ground interaction. In this case, the steady-state hitch angle where $\dot{\theta} = 0$ and its property of being the boundary value where hitch magnitude cannot decrease or increase still holds true. This assumption is used to determine θ_{cr} for the system in the presence of slip.

It is assumed that the vehicle–trailer system are backing up slowly, thus dynamic effects of the motion are neglected from the model. We first begin with the dynamic equations for the planar coupled system given in Equations (2)–(5). At steady state, the linear and rotational accelerations relative to the vehicle are zero, that is $\dot{U}_\mathrm{v} = \dot{V}_\mathrm{v} = \dot{U}_\mathrm{t} = \dot{V}_\mathrm{t} = \dot{\omega}_\mathrm{v} = \dot{\omega}_\mathrm{t} = 0$. Next, we apply our assumption that $\dot{\theta} = 0$ resulting in $\omega_\mathrm{v} = \omega_\mathrm{t} = \omega$. Finally, the system at steady state must have constant velocity and yaw rates, therefore V_v and ω are constant.

With these constraints, we can therefore solve the four nonlinear Equations (2)–(5) for the four unknowns: V_v , ω, θ and F_v , the vehicle lateral velocity, yaw rate, hitch angle and tractive force necessary at equilibrium. Manipulation of the equations and eliminating the zero terms yield the following constraint equations:

$$0 = \sum F_{x\mathrm{v}} + \sum F_{x\mathrm{t}} \cos\theta - \sum F_{y\mathrm{t}} \sin\theta + [(m_\mathrm{v} + m_\mathrm{t})V_\mathrm{v} - m_\mathrm{t}\omega(d_\mathrm{v} + d_\mathrm{t}\cos\theta)]\omega, \quad (12)$$

$$0 = \sum F_{y\mathrm{v}} + \sum F_{x\mathrm{t}} \sin\theta + \sum F_{y\mathrm{t}} \cos\theta - [(m_\mathrm{v} + m_\mathrm{t})U_\mathrm{v} + m_\mathrm{t} d_\mathrm{t}\omega \sin\theta]\omega, \quad (13)$$

$$0 = \sum M_\mathrm{v} + d_\mathrm{v}\left(\sum F_{y\mathrm{v}} - m_\mathrm{v} U_\mathrm{v}\omega\right), \quad (14)$$

$$0 = \sum M_\mathrm{t} - d_\mathrm{t}\left[\sum F_{x\mathrm{v}} \sin\theta - \sum F_{y\mathrm{v}} \cos\theta + m_\mathrm{v}\left(U_\mathrm{v}\cos\theta + V_\mathrm{v}\sin\theta\right)\omega\right]\dot{\theta}. \quad (15)$$

However, the nonlinearity of the above constraint equations allows the existence of multiple solutions. To resolve this, we minimise $|\theta|$ subject to the constraints. The simple saturation function of the lateral tyre force model (i.e. lateral force is linear with slip angle and is saturated by $F_y \leq \mu F_z$) results in conditions where variations of wheel slip angles yields exactly the same value for lateral force, causing problems in the numerical minimization solver which uses a numerical gradient method to determine optimality. To improve the solver efficacy, we implement a simplified version of the nonlinear Pacejka Magic Formula tyre model,[29] assuming that the vertical loads are constant and the slip angle is invariant to the vertical load. More specifically, we assume that the effects of load transfer due to pitch and roll are negligible as the motion is carried out slowly, however, variation in the loading condition (such as cargo location on the trailer) will change the vertical load distribution, resulting in a change in the tyre normal force F_z. Furthermore, changes in the steering input will also result in a change in the slip angle of the steered wheels. The resulting lateral force is a function of the road–tyre friction coefficient μ, the normal tyre load F_z, the tyre slip angle α:

$$F_y = -\mu F_z \sin\left(C_1 \arctan\left[\frac{C_\alpha}{C_1\mu F_z}\alpha - C_2\left\{\frac{C_\alpha}{C_1\mu F_z}\alpha - \arctan\frac{C_\alpha}{C_1\mu F_z}\alpha\right\}\right]\right). \quad (16)$$

Longitudinal forces F_x are modelled as the vehicle longitudinal driving force F_v (required to overcome the motion resistance due to tyre slip and rolling resistance) and a rolling resistance opposing the rolling motion direction, given by

$$F_x = -\mu_r F_z + F_\mathrm{v}. \quad (17)$$

Note that in these tyre models, we do not explicitly consider the effects of a deformable ground (e.g. soil dynamics). However, the Equations (12)–(15) are still valid for as long as an appropriate tyre–ground contact model, such as Equations (16) and (17) generate F_x and F_y representative of the tyre–ground interaction at hand.

The steady-state conditions are computed using the constrained minimization problem as defined above for a constant $U_\mathrm{v} = -5$ kph using Matlab's '`fmincon`' function with an 'active-set' solver algorithm. The nonlinear constraint equations are only met when all of the accelerations $\dot{U}_\mathrm{v}$, $\dot{V}_\mathrm{v}$ and $\dot{\omega}$ are zero, with $\dot{\theta} = 0$. The minimization numerically attempts to

solve for the lowest θ such that these conditions are met, however, an initial guess is necessary for the numerical solver. A selection of initial guess close to the solution improves the success rate of the numerical solver in obtaining a solution satisfying the nonlinear constraints.

In this minimization problem, the states are $x = [V_v, \omega, \theta, \dot{\theta}, F_v]$. We use a set of states satisfying the nonholonomic constraint for each δ_v as an initial guess for the solver. Derivation of the states satisfying the nonholonomic constraint, called the no-slip curve (NSC) was introduced in [27]. The NSC resides in the hitch control space, spanning the space of configuration variables $[\delta_v, \delta_t, \theta]$ for which the nonholonomic constraint is satisfied. For the single-axle trailer without steering, $\delta_t = 0$ and the initial guess state is therefore given by

$$x_0 = \left[\frac{b_v U_v \tan\delta_v}{l_v}, \frac{U_v \tan\delta_v}{l_v}, -\arctan\frac{c_v \tan\delta_v}{l_v}, 0, 0\right]$$

3.2. *Existing result: a kinematic solution for critical hitch angle of single-axle trailers*

In the previous section we have provided a framework for determining the critical hitch angle of a single-axle unsteered vehicle–trailer where tyre slip can be non-zero. Making the assumption that the motion of the vehicle and trailer satisfies the nonholonomic constraint, that is, the wheels are only able to move in their plane, one can obtain an analytical expression for θ_{cr}. In this case, the assumption effectively restricts the vehicle–trailer motion such that lateral slip of the tyre is zero. In [9] the author states the difference in hitch angle due to a vehicle displacement Δx over one time step is given by

$$\theta(t+1) = \theta(t) + 2\arcsin\left[\frac{\Delta x \sin\left[\theta(t) - \arctan(c_v/r_v)\right]}{2c_t}\right] + \frac{\Delta x}{r_H} \tag{18}$$

where $\theta(t)$ is the current hitch angle, r_v is the radius of rotation of the vehicle, r_H is the radius of rotation of the hitch point and $\theta(t+1)$ is the hitch angle after distance Δx of the vehicle, shown in Figure 9.

Assuming the vehicle motion is nonholonomic, the vehicle radius of rotation is given by $r_v = l_v/\tan\delta_v$, where l_v is the vehicle wheelbase and the kinematic relation between the radius of curvature of the vehicle hitch point r_H and the steering angle δ_v is given by

$$r_H = \mathrm{sgn}(\delta_v)\sqrt{\left(\frac{l_v}{\tan\delta_v}\right)^2 + {c_v}^2} \tag{19}$$

From Equation (18) and the radii r_v and r_H as a function of the steering angle δ_v , we can obtain the change of hitch angle at each time step $\Delta\theta = \theta(n+1) - \theta(n)$ as

$$\Delta\theta = 2\arcsin\left[\frac{\Delta x \sin\left[\theta - \arctan(c_v \tan\delta_v/l_v)\right]}{2c_t}\right] + \frac{\Delta x}{\mathrm{sgn}(\delta_v)\sqrt{(l_v/\tan\delta_v)^2 + c_v^2}} \tag{20}$$

Now that we have the equation for the change in hitch angle, the objective is to solve for the steady-state hitch angle θ_{ss} in order to determine value for which $|\theta|$ remains constant. The steady-state condition for hitch angle is given by $\Delta\theta = 0$, therefore from Equations (18) and (19) we obtain

$$\theta_{ss} = -\arcsin\left[\frac{2c_t}{\Delta x}\sin\left(\frac{\Delta x}{2r_H}\right)\right] + \arctan\frac{c_v}{r_v} \tag{21}$$

As stated in Section 2, the steady-state condition yields the boundary between increasing and decreasing hitch angles. This boundary condition therefore determines the minimum

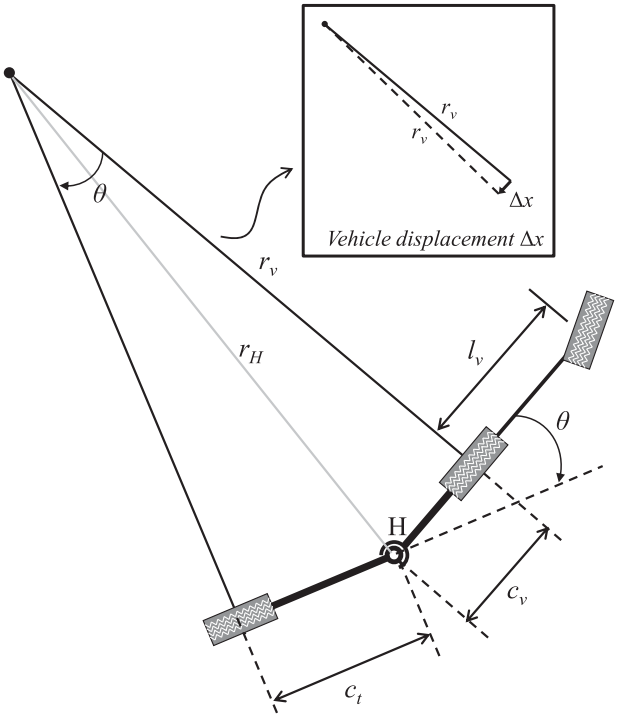

Figure 9. If it is assumed that the vehicle–trailer motion is nonholonomic, the vehicle rotates about some instantaneous centre of rotation (ICoR) with radius r_v. The radius of the hitch about this ICoR is r_H, where it is assumed the hitch is rigidly attached to the vehicle. The trailer rotates about hitch point H, with hitch angle θ relative to the vehicle. As the vehicle backs up over one time step, it moves with displacement Δx, shown in the inset. The small angle approximation results in the radius to the ICoR remain unchanged with value r_v.

hitch angle for each δ_v such that the hitch magnitude no longer decreases. The extremum values of this solution at maximum and minimum δ_v are therefore the θ_cr of the system. Since the trailer is unsteered, δ_t is constrained to a fixed value. Therefore, beyond θ_cr there does not exist any possible combination of vehicle and trailer steering angles (noting that δ_t is fixed) that can reduce the hitch angle magnitude during backing up, so therefore this is the absolute critical hitch angle $\theta_\mathrm{cr,a}$:

$$\theta_\mathrm{cr,a} = -\arcsin\left[\frac{2c_\mathrm{t}}{\Delta x}\sin\left(\frac{\Delta x}{2\mathrm{sgn}(\delta_\mathrm{v})\sqrt{(l_\mathrm{v}/\tan(\pm\delta_{v,\max}))^2 + c_\mathrm{v}^2}}\right)\right] + \arctan\frac{c_\mathrm{v}\tan(\pm\delta_{v,\max})}{l_\mathrm{v}} \tag{22}$$

The relationship between $\dot{\theta}$, δ_v and θ can also be found in [30] using similar assumptions of no-slip motion. In this work, they show that with a feedback control on the steering angle, the closed-loop response of the hitch rate can be near linear, thus lending well to analysis of stability of the closed-loop system using classical linear control methods. This approach to finding $\theta_\mathrm{cr,a}$ lends well to vehicle–trailer configurations that have kinematic or near-kinematic motion, however in a more general case (such as long-wheelbase dual-axle trailers) there may be non-trivial tyre slip that needs to be factored into the solution. In Section 3.3 we will compare the critical hitch angle for a single-axle trailer making the no-slip assumption with the result where tyre slip is present.

Table 2. Parameters for the vehicle with a single-axle trailer.

Parameter	Value (units)	Parameter	Value (units)
m_v	2000 kg	a_v	1.2 m
b_v	1.6 m	c_v	1.3 m
m_t	1800 kg	d_t	2.5 m
c_t	3.5 m	$C_{\alpha,vf}$	1250 N/°
$C_{\alpha,vr}$	1500 N/°	$C_{\alpha,tr}$	1000 N/°
C_1	1.2	C_2	–2.0

Note: The vehicle is front-steered and can steer to ±30° whereas the trailer is unsteered.

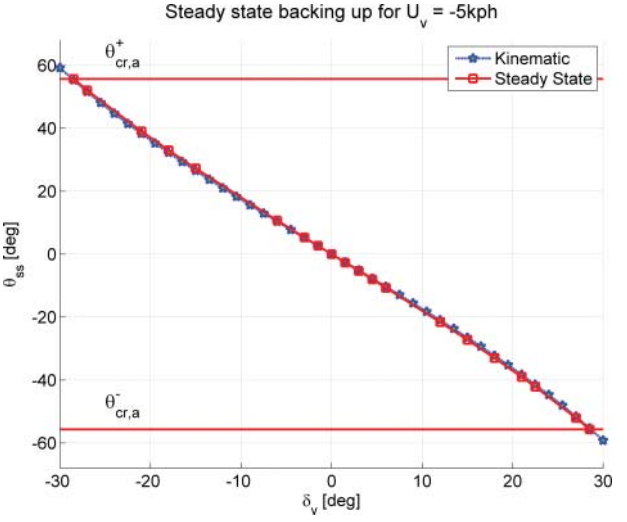

Figure 10. θ_{ss} for unsteered single-axle trailer at $U_v = -5$ kph, solved using both a kinematic analysis model and steady-state analytical approach (which makes no assumptions on the tyre slip). The kinematic solution based on no-slip kinematics results in a virtually the same steady-state hitch angle magnitude than when tyre slip is present and allowed. This suggests that the slow backing up motion of a single-axle trailer experiences very little tyre slip. $\theta^+_{cr,a}$ and $\theta^-_{cr,a}$ are the values of the steady-state solution at vehicle steering angle extrema.

3.3. *Critical hitch angle for single-axle trailers*

In this section, we assume that the hitch does not transmit any vertical loads between vehicle and trailer (also known as tongue weight) for simplification of the vehicle–trailer tyre forces. Note that as the distance from the CoM to the single-axle axis increases, the tongue weight increases accordingly. The rule of thumb for tongue weight is 10–15% of the trailer weight.[31] It may be necessary to model the tongue weight effect on tyre forces under conditions when the tongue weight is significantly larger due to improper loading of the trailer. Solving for the steady state using the tyre forces approach outlined in Section 3 for the single-axle trailer results in a slightly larger magnitude θ_{ss} than using the purely kinematic approach presented in Section 3.2. The results shown are for the vehicle–trailer parameters given in Table 2.

In Figure 10 , we superpose the solution for θ_{ss} using our analytic solver approach over the kinematic solution and demonstrate that there is very little difference in both methods for a single-axle trailer. The trivial steady-state solution at $\delta_v = 0°$ is equal for both kinematic and

numerically solved solutions since at zero steering and hitch angle, the vehicle and trailer is in a straight backward motion and thus the wheels only move in their planes. The remarkable similarity between the result using both methods demonstrates that the motion of a single-axle trailer is nearly kinematic, that is, for this type of trailer there is very little slip in the tyres when backing up is performed slowly. Furthermore, it demonstrates that our approach is viable in solving for the critical hitch angle. In situations where tyre slip is small, our proposed approach is equivalent to the kinematic analysis, which assumes from the onset that tyre slip is zero.

The solutions are very similar, but not exact. The small discrepancy between these results is due to the no-slip constraint for a purely kinematic analysis (e.g. NSC and Equation (21)) preventing lateral sliding of the tyre. However, solving for the steady state using forces and moments, we know that in order to generate any tyre forces there is a necessity of tyre slip. The θ_{ss} including necessary slip is therefore larger than if zero-slip is assumed, and the disparity between the results increases with larger velocities. With this result, we now generalise to the dual-axle trailer case, where tyre slip is not only present, but we also show why tyre slip is necessary for any non-trivial cases.

4. Critical hitch angle for dual-axle long-wheelbase trailers

4.1. *Dual-axle trailer model*

In Section 3 , we demonstrated the existing result for single-axle trailers assuming nonholonomic motion. However, when we consider dual-axle long-wheelbase trailers, there does not exist any possible solutions except the trivial one (i.e. straight forward and backward with zero steering angles) and the NSC,[27] under which the nonholonomic assumption is satisfied. In order to determine a critical hitch angle, we must take into consideration the lateral tyre slip. In Figure 11, we show the geometric and configuration parameters of a vehicle coupled to a long-wheelbase trailer with steering. The description and units of each of the vehicle–trailer parameters shown in Figure 11 are defined in Table 3.

The equations of motion for the vehicle–trailer system where the trailer has a long-wheelbase are given by

$$m_{\mathrm{v}}(\dot{U}_{\mathrm{v}} - V_{\mathrm{v}}\omega_{\mathrm{v}}) + m_{\mathrm{t}}(\dot{U}_{\mathrm{t}} - V_{\mathrm{t}}\omega_{\mathrm{t}})\cos\theta - m_{\mathrm{t}}(\dot{V}_{\mathrm{t}} + U_{\mathrm{t}}\omega_{\mathrm{t}})\sin\theta = \sum F_{x\mathrm{v}} + \sum F_{x\mathrm{t}}\cos\theta - \sum F_{y\mathrm{t}}\sin\theta, \tag{23}$$

$$m_{\mathrm{v}}(\dot{V}_{\mathrm{v}} + U_{\mathrm{v}}\omega_{\mathrm{v}}) + m_{\mathrm{t}}(\dot{U}_{\mathrm{t}} - V_{\mathrm{t}}\omega_{\mathrm{t}})\sin\theta + m_{\mathrm{t}}(\dot{V}_{\mathrm{t}} + U_{\mathrm{t}}\omega_{\mathrm{t}})\cos\theta = \sum F_{y\mathrm{v}} + \sum F_{x\mathrm{t}}\sin\theta + \sum F_{y\mathrm{t}}\cos\theta, \tag{24}$$

$$I_{\mathrm{v}}\dot{\omega}_{\mathrm{v}} + d_{\mathrm{v}} \cdot m_{\mathrm{v}}(\dot{V}_{\mathrm{v}} + U_{\mathrm{v}}\omega_{\mathrm{v}}) = \sum M_{\mathrm{v}} + d_{\mathrm{v}} \cdot \sum F_{y\mathrm{v}}, \tag{25}$$

$$I_{\mathrm{t}}\dot{\omega}_{\mathrm{t}} - d_{\mathrm{t}} \cdot m_{\mathrm{v}}[(\dot{U}_{\mathrm{v}} - V_{\mathrm{v}}\omega_{\mathrm{v}})\sin\theta - (\dot{V}_{\mathrm{v}} + U_{\mathrm{v}}\omega_{\mathrm{v}})\cos\theta] = \sum M_{\mathrm{t}} - d_{\mathrm{t}} \cdot \left(\sum F_{x\mathrm{v}}\sin\theta - \sum F_{y\mathrm{v}}\cos\theta\right), \tag{26}$$

where U_{v}, V_{v} are the longitudinal and lateral velocities of the vehicle, with vehicle yaw rate ω_{v} . The longitudinal and lateral velocities of the trailer are denoted by U_{t}, V_{t}, with trailer yaw

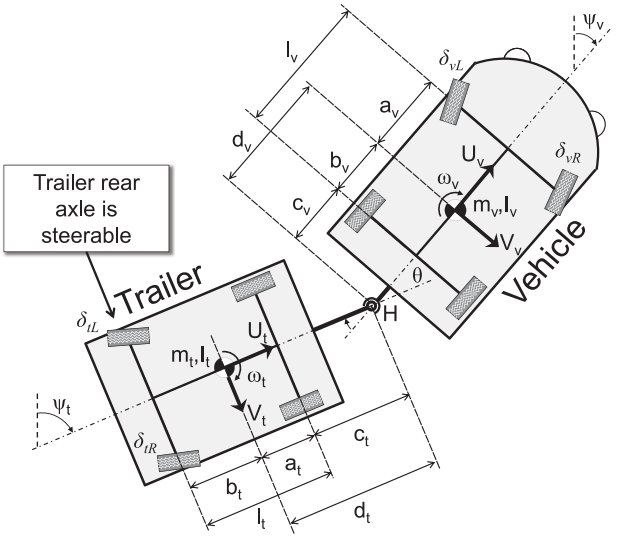

Figure 11. Dimensions for vehicle and dual-axle long-wheelbase trailer system. The vehicle has front-steered wheels and the trailer has rear-steered wheels. The vehicle has left and right steering angles $\delta_{v\mathrm{L}}$ and $\delta_{v\mathrm{R}}$, determined by Ackermann geometry, with average value δ_v. The trailer has left and right steering angles $\delta_{t\mathrm{L}}$ and $\delta_{t\mathrm{R}}$, determined by Ackermann geometry, with average value δ_t. The vehicle and trailer are connected via revolute hitch joint H.

Table 3. Vehicle and long-wheelbase trailer parameter definitions.

Parameter	Description	Units
a_v	Longitudinal distance from vehicle CoM to front axle	m
b_v	Longitudinal distance from vehicle CoM to rear axle	m
c_v	Longitudinal distance from vehicle rear axle to hitch	m
l_v	Vehicle wheelbase ($l_\mathrm{v} = a_\mathrm{v} + b_\mathrm{v}$)	m
d_v	Longitudinal distance from vehicle CoM to hitch	m
a_t	Longitudinal distance from trailer CoM to front axle	m
b_t	Longitudinal distance from trailer CoM to rear axle	m
c_t	Longitudinal distance from trailer front axle to hitch	m
l_t	Trailer wheelbase ($l_\mathrm{t} = a_\mathrm{t} + b_\mathrm{t}$)	m
d_t	Longitudinal distance from trailer CoM to hitch	m
m_v	Vehicle mass	kg
m_t	Trailer mass	kg
I_v	Vehicle yaw moment of inertia about CoM	kg m^2
I_t	Trailer yaw moment of inertia about CoM	kg m^2
δ_v	Vehicle steering angle (front), clockwise-positive	$^\circ$
δ_t	Trailer steering angle (rear), clockwise-positive	$^\circ$
$C_{\alpha,\mathrm{vf}}$, $C_{\alpha,\mathrm{vr}}$	Vehicle lateral cornering stiffness (front, rear)	N/$^\circ$
$C_{\alpha,\mathrm{tf}}$, $C_{\alpha,\mathrm{tr}}$	Trailer lateral cornering stiffness (front, rear)	N/$^\circ$

rate ω_t . For both the vehicle and trailer, we use the simplified 'bicycle model', and the tyre force terms and the corresponding moments about the vehicle and trailer CGs are given by

$$\sum F_{x\mathrm{v}} = F_{x\mathrm{v,f}}\cos\delta_\mathrm{v} - F_{y\mathrm{v,f}}\sin\delta_\mathrm{v} + F_{x\mathrm{v,r}}, \tag{27}$$

$$\sum F_{y\mathrm{v}} = F_{x\mathrm{v,f}}\sin\delta_\mathrm{v} + F_{y\mathrm{v,f}}\cos\delta_\mathrm{v} + F_{y\mathrm{v,r}}, \tag{28}$$

$$\sum M_\mathrm{v} = a_\mathrm{v}(F_{x\mathrm{v,f}}\sin\delta_\mathrm{v} + F_{y\mathrm{v,f}}\cos\delta_\mathrm{v}) - b_\mathrm{v}\cdot F_{y\mathrm{v,r}}, \tag{29}$$

Table 4. Parameters for the vehicle with a long-wheelbase dual-axle trailer.

Parameter	Value (units)	Parameter	Value (units)
m_v	2000 kg	a_v	1.2 m
b_v	1.6 m	c_v	1.3 m
m_t	1800 kg	a_t	1.0 m
b_t	1.0 m	c_t	1.5 m
$C_{\alpha,vf}$	1250 N/ °	$C_{\alpha,vr}$	1500 N/ °
$C_{\alpha,tf}$	1000 N/ °	$C_{\alpha,tr}$	1000 N/ °
C_1	1.2	C_2	−2.0

Note: The vehicle is front-steered and can steer to ±30°.

$$\sum F_{xt} = F_{xt,f} + F_{xt,r}\cos\delta_t - F_{yt,r}\sin\delta_t, \tag{30}$$

$$\sum F_{yt} = F_{yt,f} + F_{yt,r}\cos\delta_t + F_{xt,r}\sin\delta_t, \tag{31}$$

$$\sum M_t = a_t \cdot F_{yt,f} - b_t(F_{yt,r}\cos\delta_t + F_{xt,r}\sin\delta_t). \tag{32}$$

As with the case of the single-axle trailer, we use a nonlinear tyre model representative of a tyre–ground interaction on a solid surface to determine the force terms. The force of the tyre in its lateral and longitudinal directions are calculated by Equations (16) and (17).

4.2. *Critical hitch angle for unsteered dual-axle trailers*

The dual-axle long-wheelbase trailer is assumed to have a hitch that has zero tongue weight (i.e. a drawbar hitch). As previously stated, the only solution satisfying a kinematic (i.e. no-slip) constraint is the trivial solution of $\delta_v = 0°$ and $\theta_{ss} = 0°$ and the unique solutions on the NSC. It is necessary to solve for the critical hitch angle using the tyre force numerical approach similar to Equations (12)–(15) used for the single-axle trailer in Section 3.1. Once again, the approach is to minimise $|\theta|$ subject to the constraint Equations (12)–(15). As before, we utilise the same tyre–ground contact model presented in Equations (16) and (17).

The vehicle–trailer parameters that were used for this analysis are given in Table 4, assuming a fully loaded trailer with steering on the rear axle wheels. Note the long-wheelbase of the dual-axle trailer (2.0 m), which makes the behaviour of such a system significantly different from that of a single-axle trailer.

Using Matlab's '`fmincon`' function with an 'active-set' solver algorithm, we can compute the steady-state hitch angle θ_{ss} for any δ_v with $U_v = -5$ kph. The initial guess for the numerical solver is based on the nonholonomic constraint assuming a trailer without steering, given in Equation (18). In Figure 12 , we show the steady-state solutions of hitch angle for the unsteered dual-axle long-wheelbase trailer, comparing them to the kinematic solution assuming a single axle, where the effect of having a front axle is ignored completely.

In this case, we see that the kinematic solution and the steady-state solution do not match nearly as well once the front axle is introduced into the problem when compared to the similarity of both approaches when analysing the single-axle trailer in Section 3.3. The necessity for tyre slip in the dual-axle trailer under turning results in inaccuracies when using the kinematic assumption that the motion is nonholonomic. Not only is the absolute critical hitch angle higher with the non-analytical approach, but the slope of the solutions around $\delta_v = 0$ is also significantly different. As the vehicle steering angle magnitude increases, the correlation between the kinematic solution (assuming no slip motion) and the steady-state solution begins to increase. If we assume that the front tyres are allowed to move freely in both longitudinal and lateral directions (i.e. holonomically), then the system becomes kinematically

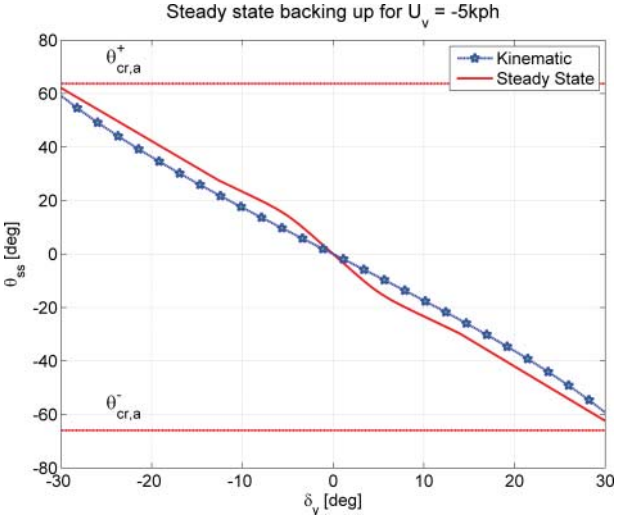

Figure 12. Solved set of steady-state hitch angles during backing up of a vehicle–trailer system with $U_{\mathrm{v}} = -5$ kph and no trailer steering. The kinematic solution shown uses the existing result from Section 3.2, effectively ignoring the front axle of the trailer.

similar to a single-axle trailer because the front axle only supports vertical loads. This suggests that at high steering angles for this parameter set, the tyres of the front axle of the trailer experiences significant lateral slip and the lateral forces are likely saturated.

4.3. *Critical hitch angle for steered dual-axle trailers*

Our main interest is the case where the driver and only the driver controls δ_{v} , and a control system actuates δ_{t} . We can characterise $\theta_{\mathrm{cr,d}}$ by the minimum and maximum θ_{ss} for all ranges of feasible trailer steering angles for a given commanded vehicle steering angle δ_{v}. In other words, for a specified δ_{v}:

$$\theta^{+}_{\mathrm{cr,d}} = \max \theta_{\mathrm{ss}}|_{\delta_{\mathrm{v}}} \quad \forall\, \delta_{t,\min} \leq \delta_{\mathrm{t}} \leq \delta_{t,\max}, \tag{33}$$

$$\theta^{-}_{\mathrm{cr,d}} = \min \theta_{\mathrm{ss}}|_{\delta_{\mathrm{v}}} \quad \forall\, \delta_{t,\min} \leq \delta_{\mathrm{t}} \leq \delta_{t,\max}. \tag{34}$$

Similarly, we can also determine the $\theta_{\mathrm{cr,a}}$ by looking at the directional critical hitch angle at the extrema vehicle steering angles. In other words:

$$\theta^{+}_{\mathrm{cr,a}} = \max \theta_{\mathrm{ss}} \begin{cases} \forall\, \delta_{t,\min} \leq \delta_{\mathrm{t}} \leq \delta_{t,\max}, \\ \forall\, \delta_{v,\min} \leq \delta_{\mathrm{v}} \leq \delta_{v,\max}, \end{cases} \tag{35}$$

$$\theta^{-}_{\mathrm{cr,a}} = \min \theta_{\mathrm{ss}} \begin{cases} \forall\, \delta_{t,\min} \leq \delta_{\mathrm{t}} \leq \delta_{t,\max}, \\ \forall\, \delta_{v,\min} \leq \delta_{\mathrm{v}} \leq \delta_{v,\max}. \end{cases} \tag{36}$$

By calculating the critical hitch angle for such a system, we are able to determine where the system must stop backing up and pull forward in order to prevent jackknifing. Furthermore, such information can also be used by the driver to quantitatively gauge how close the current operating condition is from the critical hitch angle. Using Matlab's '`fmincon`' function with an 'active-set' solver algorithm, we can compute the steady-state hitch angle θ_{ss} for any δ_{v} and δ_{t} with $U_{\mathrm{v}} = -5$ kph. We use a set of states satisfying the nonholonomic constraint for each δ_{v} as an initial guess for the solver. The initial guess state for the dual-axle long-wheelbase

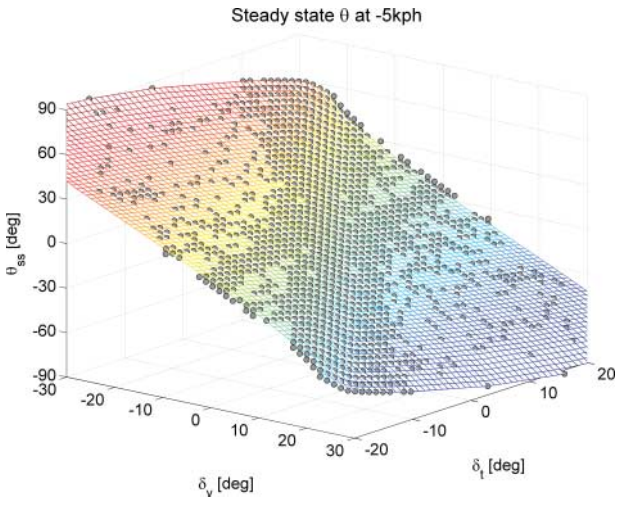

Figure 13. Solved set of steady-state hitch angles (shown as dots) during backing up of a vehicle–trailer system with $U_v = -5$ kph. A linear interpolation fitted surface matching the steady-state solution points is shown superposed, with the colours of the mesh representing the values of the steady-state hitch angles from blue being smallest to red being largest.

steered trailer used is the NSC,[27] given by

$$x_0 = \left[\frac{b_v U_v \tan\delta_v}{l_v}, \frac{U_v \tan\delta_v}{l_v}, \arctan\frac{c_t \tan\delta_t}{l_t} - \arctan\frac{c_v \tan\delta_v}{l_v}, 0, 0 \right] \tag{37}$$

In Figure 13, we show the steady-state hitch angle for $-30^\circ \leq \delta_v \leq 30^\circ$ and $-20^\circ \leq \delta_t \leq 20^\circ$ by point markers in the hitch control space. The points are used to generate a best-fit mesh surface as shown superposed. The '`fmincon`' numerical solver is unable to solve the constrained minimization problem if the initial guess state is too far from the steady-state solution. Due to the choice of initial condition for the numerical solver given in Equation (37), which is the states of the vehicle–trailer satisfying nonholonomy, we get a significantly higher success rate of solving the optimization problem along the region around the NSC.

We schematically demonstrated the curve of steady-state solutions in Figure 7(a) and 7(b) and how such information could be utilised for a backing up control strategy. We are now able to extract a steady-state solution curve by taking the intersection between the steady solution surface and the $\theta - \delta_t$ plane at each δ_v , as shown in Figure 14. In this example, we show the extraction of the steady-state solution curves for the $\delta_v = 0^\circ$ and $\delta_v = 10^\circ$ planes.

The iso-θ contours of the surface also provides some useful information regarding the possible combinations of δ_v and δ_t such that the hitch angle magnitude does not increase. Figure 15 shows the contour map of the surface shown in Figure 13, the conditions for a steady-state hitch angle. Effectively, any combination of steering inputs to the left of the iso-θ contour decreases hitch angle and any combination to the right increases it for that given initial hitch angle. For example, for a hitch angle of $\theta = 10^\circ$, any combination of δ_v and δ_t to the left of the corresponding iso-θ contour should reduce hitch angle magnitude.

Based on a trailer steering range of $-20^\circ \leq \delta_t \leq 20^\circ$, we show the upper and lower limits for $\theta_{cr,d}$ as defined by Equations (33) and (34) in Figure 16. In the $\delta_v = \pm 10^\circ$ range, $\theta_{cr,d}$ is nearly linear, however it is important to note that the solution assuming no slip does exceed the area bounded by $\theta^+_{cr,d}$ and $\theta^-_{cr,d}$ at large values of δ_v . This means as the driver gets towards the maximum and minimum steering limits of the vehicle, the ability to maintain directional

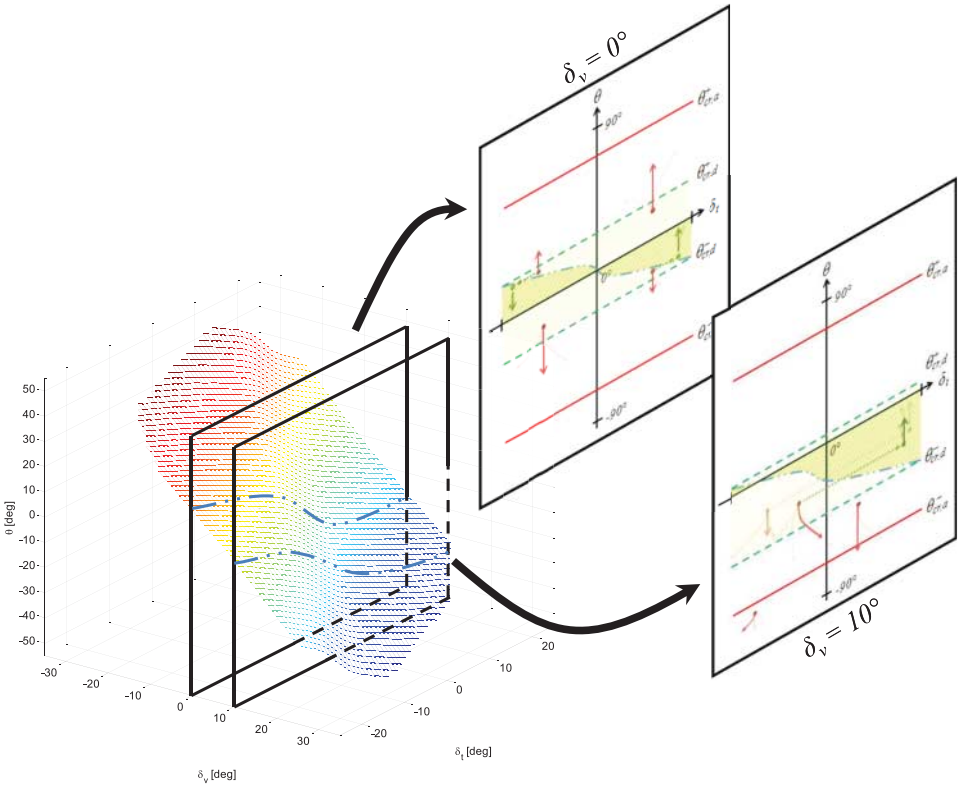

Figure 14. The steady-state solution curves are the intersections of the steady solution surface at constant δ_v planes in the hitch control space, shown for $\delta_v = 0^\circ$ and $\delta_v = 10^\circ$ planes, which were originally presented schematically in Figure 7(a) and 7(b).

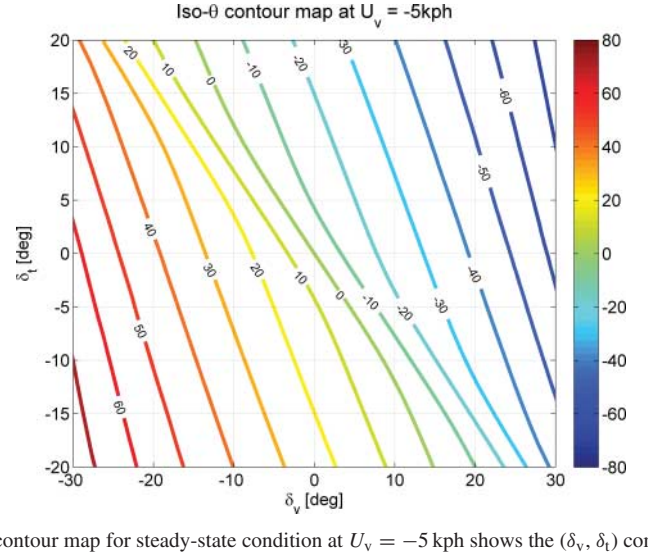

Figure 15. Iso-θ contour map for steady-state condition at $U_v = -5$ kph shows the (δ_v, δ_t) combinations for each steady-state hitch angle. For each hitch angle θ, the operating points of (δ_v, δ_t) to the left of the iso-θ contour result in $\dot{\theta} < 0$, whereas the operating points to the right of the iso-θ contour result in $\dot{\theta} > 0$.

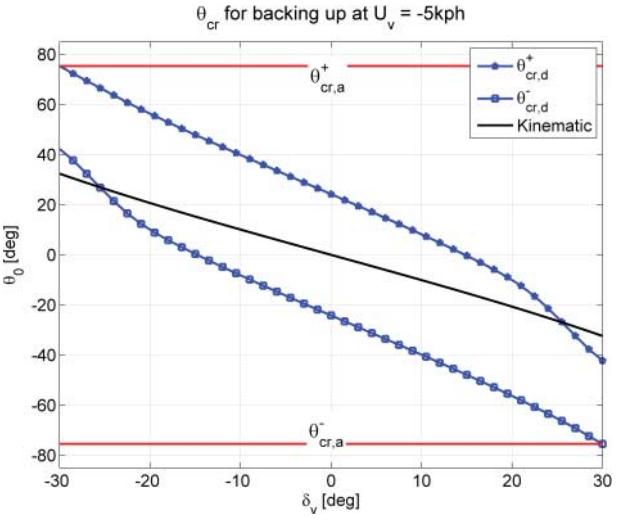

Figure 16. Calculated $\theta^{+}_{\mathrm{cr,d}}$ and $\theta^{-}_{\mathrm{cr,d}}$ for each value of δ_{v} at $U_{\mathrm{v}} = -5$ kph, where the trailer steering angle is limited to $-20^{\circ} \leq \delta_{\mathrm{t}} \leq 20^{\circ}$. For each δ_{v}, we can see the directional critical hitch angles, beyond which it is not possible for the trailer steering controller to recover and prevent jackknifing. The values of $\theta^{+}_{\mathrm{cr,a}}$ and $\theta^{-}_{\mathrm{cr,a}}$ are the maximum and minimum of $\theta_{\mathrm{cr,d}}$.

stability diminishes. The calculations also show that with a $\delta_{\mathrm{t}} = \pm 20^{\circ}$ limit, the system is not able to back up in a stable manner when δ_{v} is at the maximum/minimum values of $\pm 30^{\circ}$.

The values for $\theta_{\mathrm{cr,a}}$ is extracted from the data of $\theta^{+}_{\mathrm{cr,d}}$ and $\theta^{-}_{\mathrm{cr,d}}$ at the extreme vehicle steering angles, therefore, we have an $\theta_{\mathrm{cr,a}} = 75^{\circ}$ for the given vehicle–trailer parameter set in Table 4. This result indicates that for these system parameters and actuation constraints, if the hitch angle θ exceeds 75°, then the only way possible to reduce hitch angle is to stop backing up and pull the vehicle forward. Given this information, the driver should not attempt to continue backing up when the hitch angle exceeds the $\theta_{\mathrm{cr,a}}$.

In this section, we have demonstrated the directional and absolute critical hitch angle for a vehicle with a long-wheelbase trailer backing up at 5 kph. The quasi-static analysis neglects dynamic effects, and does not account for when the trailer motion is swinging towards the critical hitch angle with large rotational momentum. However, if we utilise the same approach to solve for the critical hitch angle at other speeds, we see that the $\theta^{+}_{\mathrm{cr,a}}$ does not change noticeably with a range of reasonable backing up speeds, given in Table 5. The variances in $\theta^{+}_{\mathrm{cr,a}}$ between the different speeds ranging from -1 to -9 kph are within the tolerances of the numerical solver accuracy. Note that since the parameters are laterally symmetric, $\theta^{+}_{\mathrm{cr,a}}$ and $\theta^{-}_{\mathrm{cr,a}}$ equal in magnitude and opposite sign.

To validate the absolute and directional critical hitch angles, we use a dynamic simulation of a vehicle–trailer system with fixed steering angles and varying initial hitch angles. The dynamic simulation model consists of an eighth-order differential equation of the vehicle–trailer planar dynamics, utilizing the Magic Formula tyre model for each tyre–ground contact. We compare initial values of hitch angle above and below the solved critical hitch angle to demonstrate the difference in hitch behaviour about this unique angle. First, we show in Figure 17 that the absolute critical hitch angle correlates well with the simulation model. In this case, the vehicle steering is set to the maximum value of $\delta_{\mathrm{v}} = -30^{\circ}$, with trailer steering angle at a maximum of $\delta_{\mathrm{t}} = -20^{\circ}$ in order to attempt to restore the hitch angle from an initial value back to zero. Any $\theta_0 > 76^{\circ}$ results in hitch angles that grow towards jackknife, and any $\theta_0 < 76^{\circ}$ results in a decreasing hitch angle. Note that the boundary value (i.e. the absolute

Table 5. The $\theta_{cr,a}$ decreases with increased backing up speed.

Speed (kph)	$\theta^{+}_{cr,a}$ (°)
−1	75.5
−3	75.5
−5	75.4
−7	75.5
−9	75.4

Note: This results in a lower possible operating range of hitch angles, and thus manoeuvrability of the trailer, with increased speed.

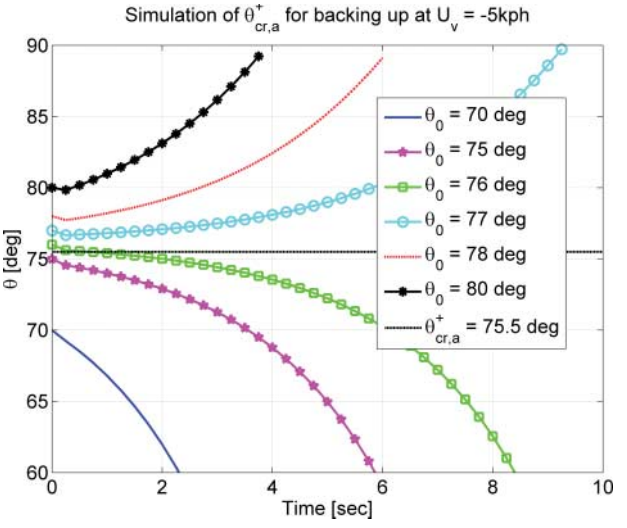

Figure 17. Simulation of the vehicle–trailer system with $\delta_v = -30^\circ$ and $\delta_t = -20^\circ$ at varying initial hitch angles to demonstrate the $\theta^{+}_{cr,a}$. Values below the absolute critical hitch angle eventually return back to zero hitch angle, but values exceeding the critical hitch angle result in an eventual jackknife.

critical hitch angle) is slightly larger than the $\theta^{+}_{cr,a} = 75.5^\circ$ as given by the numerical solver, as some small dynamic effects may be present in the simulation. In this figure, we demonstrate the direction of hitch angle for initial values θ_0 of 70°, 75°, 76°, 77°, 78° and 80°. The initial decrease in hitch angle from each θ_0, even values exceeding $\theta^{+}_{cr,a}$, is a dynamic effect caused by the initiation of the vehicle pushing on the trailer as the simulation states are initialised assuming the tyre and hitch forces on the system are zero.

5. Conclusions

We provided the formal definition of the 'critical hitch angle' (θ_{cr}) for backing up of vehicle–trailers. The critical hitch angle is *the hitch angle beyond which there exists no input steering angles δ_v (for the vehicle) and δ_t (for the trailer) that reduces the hitch angle magnitude*. For trailers with steering capability, θ_{cr} can be divided into two sub-categories: directional and absolute. We have demonstrated a systematic approach to solving for the value of θ_{cr} by presenting a set of constraints to the dynamic equations when the system is at steady state (whether stable or unstable). The θ_{cr} can be extracted from the set of steady-state solution

points to determine feasible ranges of operation for a trailer under backing up motion. We show through numerical simulation of the vehicle–trailer system that the critical hitch angle of the system does correspond to the solved value using the proposed algorithm.

Applications for use of the θ_{cr} may include advanced backing up warning systems that instruct the driver as the θ_{cr} approaches and evaluation of jackknife prevention controller performance. Such an analysis can also be utilised in the specification of trailer steering angle limits necessary on long-wheelbase trailers. In systems that allow for full driver control of vehicle steering but attempt to stabilise the system using trailer steering, such as [27], it is useful for the operator to understand the limits of the stabilisation system so as to allow for continuous backing up without resulting in jackknifing. In extreme cases, the θ_{cr} could be used to prevent jackknifing of such a system by the limitation of the vehicle steering angle until the risk of jackknifing is removed.

Our approach for solving θ_{cr} relies on the assumption that the backing up manoeuver happens at low velocity, such that the dynamic effects of the motion are neglected. It may be useful in future work to include the dynamics and look at not only the θ_{cr} as a function of the hitch control space, but also the derivative of those states. Since a constant hitch angle under backing up is only achieved in constant turns, it may be necessary to consider the effect of θ_{cr} when the hitch angle is continuously changing. Furthermore, the applicability of such system will depend on robustness due to parametric and measurement uncertainty, therefore additional work is required to fully understand the effect of these changes on the θ_{cr}.

References

[1] Fossum TV, Lewis GN. A mathematical model for trailer-truck jackknifing. SIAM Rev. 1981;23(1):95–99.
[2] Altafini C, Speranzon A, Wahlberg B. A feedback control scheme for reversing a truck and trailer vehicle. IEEE Trans Robot Autom. 2001;17(6):915–922.
[3] Balcerak E, Schikora J, Wojke P, Zobel D. Maneuver-based assistance for backing up articulated vehicles. IEEE Conference on Robotics, Automation and Mechatronics; 2004; Singapore. Vol. 2, p. 1066–1071.
[4] Bouteldja M, Koita A, Dolcemascolo V, Cadiou JC. Prediction and detection of jackknifing problems for tractor semi-trailer. IEEE Vehicle Power and Propulsion Conference. Windsor, Canada: IEEE; 2006. p. 1–6.
[5] Parra-Loera R, Corelis D. Expert system controller for backing-up a truck-trailer system in a constrained space. Proceedings of the 37th Midwest Symposium on Circuits and Systems; 1994. Vol. 2, p. 1357–1361.
[6] Deng W, Chin Y-K, Lin WC, Rule DS, Lee YH. Vehicle-trailer backing-up control system with vehicle rear wheel steering. United States Patent US 6,292,094. September 18, 2001.
[7] Ganestam P, Bengtsson N. Project in control theory – FRT090 reversing with a trailer. Technical Report. Lund, Sweden: Lund University; 2009.
[8] Lee YH, Deng W, Chin Y-K, Mckay N. Feasibility study for a vehicle-trailer backing up control. SAE International, SAE Technical Paper 2004-01-2080; 2004; Detroit, MI, USA.
[9] Shepard DR. Trailer backing up device and method. United States Patent US 7,715,953 B2. May 11, 2010.
[10] Kimmel RW. Jackknife warning system. United States Patent US 4,040,006. August 2, 1977.
[11] Kong S-G, Kosko B. Adaptive fuzzy systems for backing up a truck-and-trailer. IEEE Trans Neural Network. 1992;3(2):211–223.
[12] Tanaka K, Hori S, Wang H. Multiobjective control of a vehicle with triple trailers. IEEE/ASME Trans Mechatron. 2002;7(3):357–368.
[13] Yang X, Yuan J, Yu F. Backing up a truck and trailer using variable universe based fuzzy controller. Proceedings of the IEEE International Conference on Mechatronics and Automation; 2006; Luoyang, China. p. 734–739.
[14] Geva S, Sitte J, Willshire G. A one neuron truck backer-upper. International Joint Conference on Neural Networks; 1992; Baltimore, MD, USA. Vol. 2; p. 850–856.
[15] Zobel D, Balcerak E, Weidenfeller T. Minimum parking maneuvers for articulated vehicles with one-axle trailers. 9th International Conference on Control, Automation, Robotics and Vision; 2006; Singapore.
[16] Pradalier C, Usher K. A simple and efficient control scheme to reverse a tractor-trailer system on a trajectory. IEEE Transactions on Robotics and Automation (ICRA). Roma, Italy: IEEE; 2007. p. 2208–2214.
[17] Chen G, Zhang D. Backing up a truck-trailer with suboptimal distance trajectories. Proceedings of the Fifth IEEE International Conference on Fuzzy Systems; 1996; New Orleans, LA. Vol. 2; p. 1439–1445.
[18] Deng W, Lee YH, Yuen-Kwok C. Vehicle-trailer backing up jackknife detection and warning system. United States Patent US 6,838,979. January 4, 2005.
[19] Gonzlez-Cantos A, Ollero A. Backing-up maneuvers of autonomous tractor-trailer vehicles using the qualitative theory of nonlinear dynamical systems. Int J Robot Res. 2009;28:49–65.

[20] Koza JR. A genetic approach to finding a controller to back up a tractor-trailer truck. American Control Conference; 1992; Chicago, IL, USA. p. 2307–2311.
[21] Deng W, Lee YH. Anti-jackknife control for vehicle-trailer backing up using rear-wheel steer control. United States Patent US 6,854,557. February 15, 2005.
[22] Gonzalez-Cantos A, Maza J, Ollero A. Design of a stable backing up fuzzy control of autonomous articulated vehicles for factory automation. Proceedings of the 8th IEEE International Conference on Emerging Technologies and Factory Automation; 2001; Antibes-Juan les Pins, France. Vol. 1; p. 447–451.
[23] Yi J, Yubazaki N, Hirota K. Backing up control of truck-trailer system. IEEE International Conference on Fuzzy Systems; 2001; Melbourne, Australia. Vol. 1; p. 489–492.
[24] Matsushita K, Murakami T. Nonholonomic equivalent disturbance based backward motion control of tractor-trailer with virtual steering. Annual Conference of IEEE Industrial Electronics Society; 2005; Raleigh, NC, USA.
[25] Stergiopoulos J, Manesis S. Anti-jackknife state feedback control law for nonholonomic vehicles with trailer sliding mechanism. Int J Syst Contr Comm. 2009;1(3):297–311.
[26] Leng Z, Minor MA. A simple tractor-trailer backing control law for path following with side-slope compensation. ICRA '11. Shanghai, China: IEEE; May 2011. p. 2386–2391.
[27] Chiu J, Goswami A. Driver assist for backing-up a vehicle with a long-wheelbase dual-axle trailer. International Symposium on Advanced Vehicle Control (AVEC). Seoul, Korea: KSAE; September 2012.
[28] Fantoni I, Lozano R. Non-linear control for underactuated mechanical systems. London: Springer; 2001.
[29] Pacejka HB. Tire and vehicle dynamics, 2nd ed. Warrendale, PA: SAE International; 2006.
[30] Pradalier C, Usher K. Robust trajectory tracking for a reversing tractor trailer. J Field Robot. 2008;25(6–7):378–399.
[31] U-Haul. Towing glossary. [cited 2013 May 28]. Available from: http://www.uhaul.com/Trailers/HitchGlossary/